ISSN 1066-3622, Radiochemistry, 2019, Vol. 61, No. 6, pp. 707–713. © Pleiades Publishing, Inc., 2019.
Russian Text © The Author(s), 2019, published in Radiokhimiya, 2019, Vol. 61, No. 6, pp. 501–506.

Sorption of ^{90}Sr onto Manganese Oxides Prepared in Aqueous-Ethanol Media

A. I. Ivanets*[a], V. V. Milyutin[b], V. G. Prozorovich[a], T. F. Kuznetsova[a], A. O. Petrovskaya[a], and N. A. Nekrasova[b]

[a] *Institute of General and Inorganic Chemistry, National Academy of Sciences of Belarus, ul. Surganova 9/1, Minsk, 220072 Belarus*

[b] *Frumkin Institute of Physical Chemistry and Electrochemistry, Russian Academy of Sciences, Leninskii pr. 31, korp. 4, Moscow, 119071 Russia*

**e-mail: andreiivanets@yandex.ru*

Received October 29, 2018; revised April 18, 2019; accepted April 29, 2019

Abstract—Sorbents based on manganese oxides were prepared by $KMnO_4$ reduction in aqueous-ethanol medium. The influence of the synthesis conditions (temperature and time of the sol–gel synthesis, type of structure-forming cations, calcination temperature) on the pore structure and on the performance and selectivity in ^{90}Sr sorption was studied. The sorbents have the mesoporous structure with the specific surface area of 180–220 $m^2\ g^{-1}$ and mean pore size of 10–20 nm. Manganese oxide of channel structure in the Na^+ form, prepared by the reaction at 25°C for 5 h and heat-treated at 350°C, exhibits the highest performance and selectivity in ^{90}Sr sorption (distribution coefficient $K_d = 1.04 \times 10^4$ $cm^3\ g^{-1}$, Sr–Ca separation factor $D_{Sr/Ca} = 99$). The sorbents synthesized exhibit the highest performance and selectivity in neutral and alkaline media.

Keywords: manganese oxides, synthesis, aqueous-ethanol media, sorption, strontium, liquid radioactive waste

DOI: 10.1134/S1066362219060110

Objects associated with operation of nuclear power facilities are potentially hazardous for the population and environment. Operation of nuclear power plants and nuclear power facilities on ships and submarines results in formation of large amounts of liquid radioactive waste (LRW) requiring utilization (removal of radionuclides and their reliable disposal). ^{90}Sr is one of the most hazardous radionuclides; its half-life is relatively long, 28.5 years [1–3].

Various physicochemical methods were suggested for removing radionuclides from aqueous media. These include chemical or electrochemical deposition, ion exchange, membrane separation, adsorption, etc. [4–6]. Adsorption remains a widely used method owing to its efficiency and easy implementation. The development of highly selective ion-exchange materials for removing radionuclides from liquid radioactive waste remains a complex problem, because radionuclides are usually present in trace concentrations against the background of high concentrations of concomitant ions competing with radionuclides in sorption processes [7].

Porous inorganic materials are particularly interesting owing to their specific properties and structural diversity [8]. Mixed-valence manganese oxides with tunnel and layered structures form a large class of porous materials with the pore size from micropores to mesopores. Because these oxides demonstrate high cation-exchange properties, they can be used as ionic and molecular sieves [9, 10]. The structures of manganese oxides are built of MnO_6 octahedra. Combination of the MnO_6 octahedra by sharing common faces results in the formation of a layered structure, e.g., birnessite (the interlayer spacing is in the range 7.4–8.0 Å depending on structure-forming cations or molecules) [11]. The MnO_6 octahedra in the channel structures are combined by sharing common faces and vertices. The channel size in various structures is different. For example, in the cryptomelane structure there are 2 × 2 channels (4.6 Å) [12, 13], whereas in the todorokite structure there are 3 × 3 channels (6.9 Å) in which Mg^{2+} ions are located [14].

Sorbents based on manganese oxides are prepared most frequently by the reduction of MnO_4^- ions in

aqueous or organic media [15–18]. Mesoporous manganese oxides were prepared previously by the sol–gel method (reduction of $KMnO_4$ with polyvinyl alcohol); they showed high performance in sorption of stable strontium ions and of ^{85}Sr radionuclides from aqueous solutions. It was found that the samples contained large amounts of carbon-containing pyrolysis products of polyvinyl alcohol, negatively affecting the sorption performance and selectivity [19].

This study was aimed at preparing sorbents based on manganese oxide by the reduction of $KMnO_4$ in aqueous-ethanol medium and at determining their performance and selectivity in the ^{90}Sr sorption. The use of ethanol as reductant allows controlled reduction of $KMnO_4$ under mild conditions and complete removal of organic oxidation products in the step of the hydrogel washing.

EXPERIMENTAL

Hydrogels of manganese oxides are prepared by the sol–gel method allowing control of the composition and structure of the oxides obtained by varying the sol and gel formation conditions. 96% ethanol was added to a 1.0 wt % $KMnO_4$ solution ($KMnO_4$: EtOH weight ratio 1 : 10). The synthesis was performed in a rotary evaporator at 25°C for 5 h (series 1) and at 80°C for 48 h (series 2). The hydrogel obtained was filtered off and washed with distilled water to remove excess electrolytes to neutral pH value. Then, a portion of the hydrogel was heat-treated at 150°C for 5 h. The hydrogel preliminarily kept for 24 h in aqueous solutions containing 0.1 M K^+, Na^+, Mg^{2+}, and Ca^{2+} was heat-treated for 5 h at 350°C. The initial solutions were prepared using distilled water and chemically pure grade chemicals: $KMnO_4$, KCl, $MgCl_2 \cdot 6H_2O$, NaCl, and $CaCl_2 \cdot 6H_2O$ (Five Oceans, Belarus).

X-ray diffraction analysis of samples was performed with a DRON-3 diffractometer in monochromated CuK_α radiation at reflection angles 2θ from 20° to 80°. The surface structure, morphology, and elemental composition of the materials obtained were examined with a JSM-5610 LV scanning electron microscope equipped with an EDX JED-2201 JEOL point chemical analysis system (Japan), after preliminary vacuum sputtering of gold onto the sample surface.

The adsorption properties and texture of the samples were estimated from the isotherms of low-temperature (–196°C) physical adsorption–desorption of nitrogen. The isotherms were taken by the volumetric method with an ASAP 2020 MP analyzer of surface area and porosity (Micromeritics, the United States). The specific surface area was determined by the BET method (A_{BET}). The adsorption pore volume ($V_{sp,ads}$, $V_{sp,des}$) and the adsorption mean pore diameter ($D_{sp,ads}$, $D_{sp,des}$) were calculated by the one-point method. Prior to analysis, the samples were heat-treated for 1 h in a vacuum (150°C, 133×10^{-3} Pa).

The sorption characteristics of the manganese oxides obtained were studied at the Laboratory of Chromatography of Radioactive Elements, Frumkin Institute of Physical Chemistry and Electrochemistry, Russian Academy of Sciences. Prior to use, the samples were ground in a mortar to the particle size smaller than 0.2 mm and dried in air to constant weight at 80°C. The sorption characteristics of the samples were determined for macroamounts of Ca^{2+} and tracer amounts of ^{90}Sr as an example. Experiments were performed in the batch mode by stirring a 0.1-g portion of the air-dry sorbent with 0.02 dm^3 of the solution for 48 h. As a liquid phase we used a model 0.01 M $CaCl_2$ solution (pH 6.0) spiked with ^{90}Sr (about 10^5 Bq dm^{-3}). Then, the mixture was filtered, and the concentration of Ca^{2+} ions and activity concentration of ^{90}Sr in the filtrate were determined. From the analysis results, we calculated the static exchange capacity (SEC) for Ca^{2+}, distribution coefficient (K_d) of ^{90}Sr, and Sr/Ca separation factor ($D_{Sr/Ca}$), using formulas (1)–(3), respectively:

$$SEC = (C_0 - C_e)V_L/m_s \quad (1)$$

$$K_d = (A_0 - A_e)V_L/(A_e m_s), \quad (2)$$

$$D_{Sr/Ca} = K_d C_e/SEC, \quad (3)$$

where C_0 and C_e are the Ca^{2+} concentrations in the initial solution and filtrate, respectively, M; A_0, and A_e, activity concentrations of ^{90}Sr in the initial solution and filtrate, respectively, Bq dm^{-3}; V_L, liquid phase volume, cm^3; and m_s, sorbent weight, g.

To determine the dependence of $K_d(^{90}Sr)$ on pH of the liquid phase, we added a 1 M HNO_3 or NaOH solution to an 0.1 M $NaNO_3$ solution. The equilibrium pH values were determined with an Ekotest 2000 pH meter.

The following sorbents were tested under similar conditions for comparison:

(1) MDM, sorbent based on modified manganese dioxide, TU (Technical Specification) 2641-001-51255813-2007, semicommercial batch, produced by the Frumkin Institute of Physical Chemistry and Electrochemistry, Russian Academy of Sciences;

(2) Termoxid-3K, spherogranulated sorbent based on hydrated titanium and zirconium oxides, TU 2641-014-12342266-04, commercial batch, produced by Termoxid Research and Production Company (Zarechnyi, Sverdlovsk oblast, Russia);

(3) NaA, synthetic zeolite of type A, TU 2163-003-15285215-2006, commercial batch, produced by Ishimbai Special Chemical Catalyst Plant (Bashkortostan, Russia);

(4) S-N 103, synthetic titanosilicate, an analog of ivanyukite natural mineral, laboratory sample, synthesized at the Nanomaterials Science Center, Kola Scientific Center, Russian Academy of Sciences (Apatity, Murmansk oblast, Russia);

(5) CL, natural clinoptilolite from Shivertui deposit (Chita oblast, Russia);

(6) KU-2×8, strongly acidic sulfonic cation-exchange resin, commercial batch, produced by Tokem Research and Production Association (Kemerovo, Russia).

The activity concentration of ^{90}Sr in solutions was determined by the direct radiometric method using SKS-50M spectrometric complex (Green Star Technologies, Russia) after sample standing for no less than 10 days. The concentration of Ca^{2+} ions in solutions was determined by volumetric complexometric titration.

RESULTS AND DISCUSSION

The results of the X-ray diffraction analysis show that all the samples have the amorphous structure. Therefore, their phase composition cannot be identified by this method. Therefore, we performed IR spectroscopic analysis of the samples (Fig. 1).

As can be seen, in all the IR spectra there are peaks at 1580–1585 cm^{-1}, characteristic of stretching vibrations of OH groups bound to Mn atoms of the crystal lattice. The intensity of the peaks in this region depends on the synthesis conditions insignificantly. The bands at 400–800 cm^{-1} can be assigned to characteristic vibrations of Mn^{4+}–O bonds in manganese oxides.

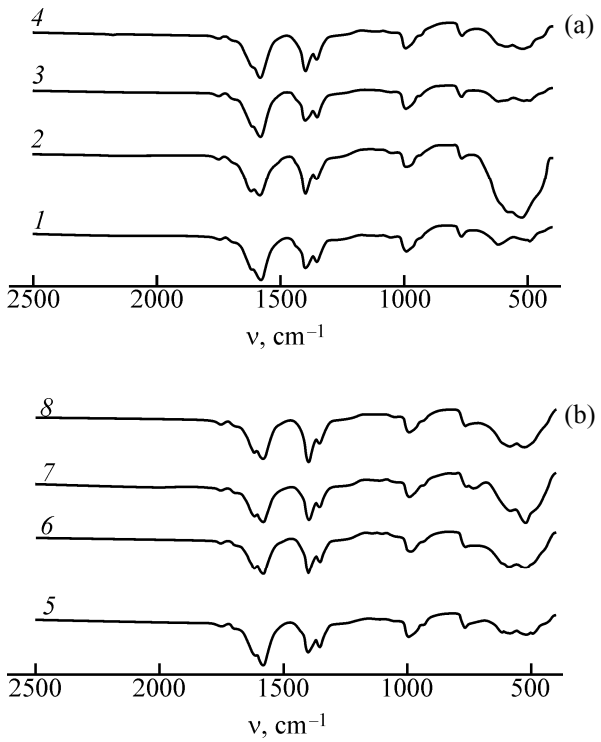

Fig. 1. IR spectra of manganese oxides obtained under different synthesis conditions. The numbering corresponds to samples in Table 1. Sample nos.: (a) 1–4 and (b) 5–8.

The absorption band at 770–760 cm^{-1} is characteristic of manganese oxides with the tunnel structure and is present in the IR spectra of all the samples [20]. The position and intensity of the absorption bands significantly differ for samples 1–4, suggesting different types of Mn–O bonds depending on the synthesis conditions. The intensity of the characteristic absorption band of the tunnel structure of manganese oxides (770 cm^{-1}) for these samples does not vary noticeably. With an increase in the synthesis time at a constant temperature of 25°C, the IR spectra remain virtually unchanged (samples 1 and 3, Fig. 1a). On the other hand, for samples 3 and 4 an increase in the synthesis temperature at a time of 48 h leads to an increase in the peak intensity at 400–650 cm^{-1}, accompanied by the shift of the strongest peaks in the interval 490–630 cm^{-1} into a narrower interval, 520–590 cm^{-1}.

Based on the results of preliminary studies, sample 4 was taken as the initial sample for preparing sorbents based on manganese oxides. Introduction of single-charged K^+ and Na^+ cations into the structure of manganese oxides (samples 5 and 6, Fig. 1b) does not lead to significant changes in the intensities and posi-

Table 1. Adsorption properties of manganese oxides

Sample	Synthesis conditions/ionic form	A_{BET}, $m^2\ g^{-1}$	$V_{sp.ads}$, $cm^3\ g^{-1}$	$V_{sp.des}$, $cm^3\ g^{-1}$	$D_{sp.ads}$, nm	$D_{sp.des}$, nm
1	5 h, 25°C	208	0.484	0.523	10	11
2	5 h, 80°C	188	0.466	0.503	10	11
3	48 h, 25°C	275	0.431	0.415	7	6
4	48 h, 80°C	284	0.623	0.621	9	9
5[a]	K^+	231	1.01	1.10	19	20
6[a]	Na^+	293	1.14	1.25	17	18
7[a]	Mg^{2+}	213	0.843	0.970	16	19
8[a]	Ca^{2+}	222	1.03	1.08	19	20

[a] Samples obtained from sample 4.

tions of the characteristic IR bands. Introduction of Na^+ ions (sample 6) leads to an increase in the intensity of the Mn–O absorption bands without their shift. On introducing Mg^{2+} ions (sample 7, Fig. 1b), the intensity of the peaks at 400–650 cm^{-1} slightly increases. In this case, the characteristic peak at 765 cm^{-1} has a shoulder at 731 cm^{-1}, which is probably associated with structural transformations. In the case of introducing Ca^{2+} ions into the structure of manganese oxide (sample 8, Fig. 1b), the IR spectrum of the sample is similar to that of the Na-containing sample (sample 6, Fig. 1b), suggesting similar structure of these samples.

Data on low-temperature nitrogen adsorption–desorption (Table 1) suggest that samples 1–4 and 5–8 of manganese oxides have different structure. For samples 1–4, the most significant changes in the adsorption properties occur with an increase in the synthesis temperature from 25 to 80°C and in the synthesis time from 5 to 48 h. As compared to sample 1, for sample 4 the specific surface area increases by a factor of 1.4 and the pore volume, by a factor of 1.2–1.3. The main differences between samples 1–4 and 5–8 consist in the coalescence of mesopores and in an increase in the pore volume with considerably less pronounced change in the specific surface area.

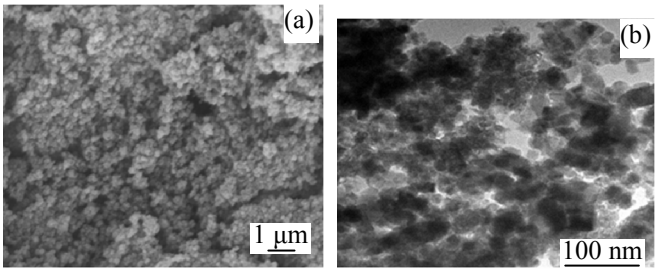

Fig. 2. (a) SEM and (b) TEM images of manganese oxide synthesized at 25°C for 5 h with the subsequent heat treatment at 150°C.

Comparison of samples 5–8 with sample 4 shows that, in the case of introduction of K^+ ions (sample 5), the values of $V_{sp,ads}$, $V_{sp,des}$ and $D_{sp,ads}$, $D_{sp,des}$ increase by a factor of 1.6–1.8 and 2.0–2.2, respectively. Similar dependence is observed on introducing Na^+ (sample 6), Mg^{2+} (sample 7), and Ca^{2+} ions (sample 8). The specific surface area either does not change (sample 6) or slightly decreases (by a factor of 1.2–1.3 for the other samples). Introduction of single- and double-charged ions acting as the structure-forming cations favors the formation of structures with the preset type of ordering for the synthesized manganese oxides.

Layered manganese oxides (samples 1–4) have similar morphology. Typical SEM and TEM images are shown in Fig. 2 for the sample synthesized at 25°C for 5 h and heat-treated at 150°C as example. The samples have pronounced globular structure with the 100–200 nm size of spherical particles (Fig. 2a). The TEM data (Fig. 2b) show that the globules are agglomerates of finer particles of 5–10 nm size.

Data of energy-dispersive X-ray analysis (Table 2) allow estimation of the content of main elements in the manganese oxide samples obtained. Irrespective of the synthesis conditions, all the samples contain approximately equal amount of Mn, 65 ± 5 at. %. High content of K^+ ions in samples 1 and 4 should be noted. These ions occur in the interlayer space and in channels of manganese oxide structures and are accessible to ion exchange in the course of sorption of polyvalent metal ions. EDX analysis shows that the content of K^+ ions in the samples decreases with an increase in the synthesis time and temperature, which should affect the ion-exchange capacity of these samples. It should be

Table 2. EDX data for manganese oxide samples

Sample	Synthesis conditions/ionic form	Element content, at. %			
		Mn	O	K	metal introduced
1	5 h, 25°C	58.6	32.3	9.1	–
4	48 h, 80°C	66.3	27.2	6.5	–
5	K^+	61.1	32.5	6.4	–
6	Mg^{2+}	68.8	27.2	1.4	2.6
7	Na^+	63.0	33.9	2.1	1.0
8	Ca^{2+}	64.0	31.0	1.8	3.2

Table 3. Static exchange capacity (SEC) for Ca^{2+}, distribution coefficient (K_d) of ^{90}Sr, and Sr/Ca separation factor ($D_{Sr/Ca}$) for manganese oxide samples (0.01 M $CaCl_2$, pH 6.0, S : L = 1 : 200)

Sample	t, h	$T_{sol-gel}/T_{heat}$, °C	Ionic form	SEC for Ca^{2+}, mmol g^{-1}	$K_d(^{90}Sr) \times 10^{-3}$, $cm^3\ g^{-1}$	$D_{Sr/Ca}$
1	5	25/150	K^+	0.85	0.75	5.6
2		25/350	Na^+	0.74	10.6	99
3			Ca^{2+}	<0.01	5.77	–
4	48	80/150	K^+	0.24	1.23	48
5		80/350	Na^+	0.44	3.83	66
6			Ca^{2+}	–	2.89	67
MDM	–	–	Na^+, K^+	0.96	8.59	56
Termoxid-3K	–	–	Na^+	0.23	0.22	8.9
NaA			Na^+	1.65	4.40	5.7
S-N 103			Na^+	1.20	23.0	92
CL			Na^+	0.34	0.31	4.6
KU-2×8			Na^+	1.80	0.22	1.4

noted that the samples prepared by conversion of the K^+ form of manganese oxides to other M^{n+} forms have the residual content of K^+ ions about 2–4 at. %, suggesting the presence of these cations in different forms with different mobility, so that a part of the K^+ cations are not involved in the ion exchange.

Comparison of the sorption-selective properties of the manganese oxides prepared and of other inorganic sorbents shows that the sorbents based on manganese oxides in the K^+ form with the tunnel structure and sorbents MDM and S-N 103 exhibit the best characteristics in the ^{90}Sr sorption (Table 3). Samples with the channel structure (1, 4) exhibit higher sorption performance and selectivity than layered samples (2, 3, 5, 6) do.

No direct correlation is observed between SEC and K_d. This is due to the fact that the exchange capacity is determined at macroconcentrations of Ca^{2+} cations, whereas the distribution coefficient characterizes the affinity of the sorbent for ^{90}Sr at microconcentrations. Analysis of the K_d and $D_{Sr/Ca}$ values for channel manganese oxides shows that the kind of the introduced cation does not significantly influence the sorption-selective characteristics.

Real liquid radioactive waste is often characterized by increased content of Ca^{2+} and Mg^{2+} ions. Therefore, determination of the effect of hardness ions on the sorption characteristics of the sorbents is of considerable practical interest. An increase in the Ca^{2+} concentration leads to a significant decrease in K_d both for sample 6 (Table 1) and for the reference MDM sample. The most pronounced decrease in the sorption-selective characteristics occurs already in the presence of 0.02 M Ca^{2+}, which is caused by competing sorption of Ca^{2+} ions whose chemical properties are close to those of Sr^{2+} (Fig. 3).

The effect of pH on K_d is more complex. Three well-defined portions are observed in the pH depend-

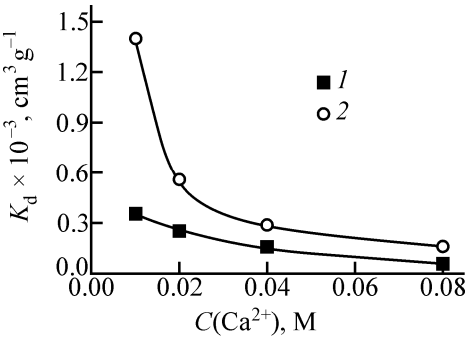

Fig. 3. Distribution coefficient (K_d) of ^{90}Sr as a function of the concentration of Ca^{2+} ions for (*1*) sample 6 from Table 1 and (*2*) MDM.

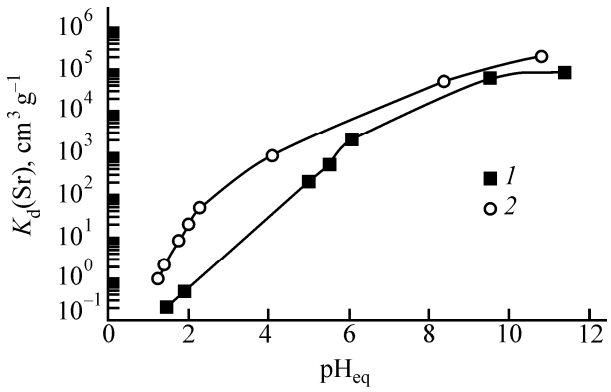

Fig. 4. Distribution coefficient (K_d) of ^{90}Sr as a function of pH of the equilibrium liquid phase for (*1*) sample 6 from Table 1 and (*2*) MDM.

ence of K_d for MDM sorbent and sample 6 (Fig. 4). Low sorption-selective characteristics at pH < 2.0 are caused by competing sorption of H^+ and Sr^{2+} ions, and also by partial dissolution of the sorbents based on manganese oxides in strongly acidic solutions. A significant increase in K_d at pH 5–6 occurs owing to the change in the sign of the sorbent surface charge from positive to negative in the zero-charge point, pH_{zcp} 5.6–5.8 [21]. In alkaline media, the pH dependence of K_d flattens out, which is caused by the onset of hydrolysis of Sr^{2+} ions and by decreased electrostatic interaction of the sorbent with the hydroxo complexes formed, $SrOH^+$.

Thus, we prepared ^{90}Sr sorbents based on mesoporous manganese oxides with high specific surface area (180–290 m^2 g^{-1}) by the sol–gel method via reduction of $KMnO_4$ in aqueous-ethanol medium. The samples prepared at 25°C for 5 h exhibit higher ion-exchange capacity for Ca^{2+} compared to the sorbents prepared at 80°C for 48 h. The materials obtained efficiently take up ^{90}Sr from aqueous solutions (the distribution coefficient reaches 4.89×10^4 cm^3 g^{-1}, and the Sr/Ca separation factor reaches 99). Irrespective of the conditions for preparing manganese oxides, Ca^{2+} ions exert a negative effect on the ^{90}Sr sorption. The sorbents show the highest performance in neutral and alkaline solutions. Comparative analysis of the sorption performance and selectivity of the manganese oxides obtained and a series of commercially available sorbents demonstrated good prospects for using our sorbents for liquid radioactive waste decontamination from ^{90}Sr.

CONFLICT OF INTEREST

The authors declare that they have no conflict of interest.

REFERENCES

1. Vellingiri, K., Kim, K.-H., Pournara, A., et al., *Prog. Mater Sci*., 2018, vol. 94, pp. 1–67.
2. Markitanova, L.I., *Nauch. Zh. Nats. Issled. Univ. Inform. Tekhnol., Mekh. Opt., Ser.: Ekon. Ekol. Menedzh.*, 2015, no. 1, pp. 140–146.
3. *Inform. Byull. Ob"ed. Inst. Energ. Yadern. Issled. – Sosny, Ser.: At. Energet.*, 2010, no. 10–11 (16–17), pp. 1–8.
4. Fang, X., Xu, Zh., Luo, Ya., et al., *Procedia Environ. Sci*., 2016, vol. 31, pp. 375–381.
5. Fedorova, V.M., Kobets, S.A., Puzyrnaya, L.N., et al., *Radiochemistry*, 2017, vol. 59, no. 5, pp. 495–499.
6. Chu, Zh., Liu, J., and Han, Ch., *Chin. J. Chem. Eng*., 2015, vol. 23, no. 10, pp. 1620–1626.
7. Milyutin, V.V., Nekrasova, N.A., Yanicheva, N.Yu., et al., *Radiochemistry*, 2017, vol. 59, no. 1, pp. 65–69.
8. Alby, D., Charnay, C., Heran, M., et al., *J. Hazard. Mater*., 2018, vol. 344, pp. 511–530.
9. Wu, M.H., Shi, J., and Deng, H.P., *Arab. J. Chem*., 2018, vol. 11, pp. 924–934.
10. Dharmarathna, S., King'ondu, C.K., Suib, S.L., et al., *Appl. Catal. B*, 2014, vol. 147, pp. 124–131.
11. Wu, Y., Feng, R., Song, Ch., et al., *Catal. Today*, 2017, vol. 281, part 3, pp. 500–506.
12. Ling, F.T., Post, J.E., and Heaney, P.J., *Chem. Geol*., 2018, vol. 479, pp. 216–227.
13. Selvaraj, A.R., Rajendiran, R., Chinnadurai, D., et al., *Electrochim. Acta*, 2018, vol. 283, pp. 1679–1688.
14. Lee, J., Ju, J.B., Cho, W.I., et al., *Electrochim. Acta*, 2013, vol. 112, pp. 138–143.

15. Ivanets, A.I., Kuznetsova, T.F., and Prozorovich, V.G., *Russ. J. Phys. Chem. A*, 2015, vol. 89, no. 3, pp. 481–485.
16. Ivanets, A.I., Prozorovich, V.G., Kouznetsova, T.F., et al., *Environ. Nanotechnol. Monit. Manag*., 2016, vol. 6, pp. 261–269.
17. Ivanets, A.I., Prozorovich, V.G., Krivoshapkina, E.F., et al., *Russ. J. Phys. Chem. A*, 2017, vol. 91, no. 8, pp. 1486–1492.
18. Egorin, A., Sokolnitskaya, T., Azarova, Yu., et al., *J. Radioanal. Nucl. Chem*., 2018, vol. 317, no. 1, pp. 243–251.
19. Ivanets, A.I., Katsoshvili, L.L., Krivoshapkin, P.V., et al., *Radiochemistry*, 2017, vol. 59, no. 3, pp. 264–271.
20. Kang, L., Zhang, M., Liu, Z.-H., et al., *Spectrochim. Acta, Part A*, 2007, vol. 67, pp. 864–869.
21. Ivanets, A.I., Prozorovich, V.G., Kouznetsova, T.F., et al., *J. Radioanal. Nucl. Chem*., 2018, vol. 316, pp. 673–683.

Translated by G. Sidorenko